# A Loose Cage for Transition Metals

**Giancarlo De Santis,[1a] Luigi Fabbrizzi,*[,1b] Angelo Perotti,[1b] Nicola Sardone,[1c] and Angelo Taglietti[1b]**

Dipartimento di Scienze, Università G. d'Annunzio, I-65127 Pescara, Italy, and Dipartimento di Chimica Generale and Centro Grandi Strumenti, Università di Pavia, I-27100 Pavia, Italy

*Received August 2, 1996*[⊗]

The octamine cage **5**, L, incorporates $Ni^{II}$, $Cu^{II}$, and $Zn^{II}$ in aqueous solution by a fast and reversible process. Equilibrium studies indicated the formation of metal complexes of protonated forms of the ligands, i.e. $M^{II}(LH_2)]^{4+}$ and $[M^{II}(LH)]^{+}$, and of the neutral ligand, $[M^{II}(L)]^{2+}$. The crystal structure of a complex of the monoprotonated ligand, $[Ni^{II}(LH)](ClO_4)_3$, has been determined by single-crystal X-ray crystallography. The complex salt ($C_{18}H_{43}N_8Cl_3NiO_{12}\cdot H_2O$) crystallizes in the orthorombic *Pbca* space group, with cell constants $a = 14.173(2)$ Å, $b = 14.383(1)$ Å, $c = 30.622(3)$ Å, $V = 6242(1)$ Å$^3$, and $Z = 8$. The $Ni^{II}$ ion is coordinated to six of the eight available nitrogen atoms, in a very distorted octahedral stereochemistry: of the two uncoordinated donor atoms, a tertiary nitrogen atom and an adjacent secondary one, it is the latter that is protonated. The easy access of protons to uncoordinated amine groups of the cage accounts for the fast demetalation of $[Ni^{II}(L)]^{2+}$ and $[Cu^{II}(L)]^{2+}$ in acidic solution, which was investigated by stopped-flow spectrophotometry. Dependence of $k_{obs}$ upon $[H^+]$ for $[Ni^{II}(L)]^{2+}$ and upon $[H^+]^2$ for $[Cu^{II}(L)]^{2+}$ indicated that the protonation of uncoordinated nitrogen atoms of the cage is the key step of the demetalation process.

## Introduction

Macropolycyclic multidentate ligands are called *cages* because of their shape and because they are able to host one or more guests (e.g. metal ions), sometimes preventing any possibility of escape. The most famous polyamine cages are sepulchrand[2] (**1**) and sarcophagine[3] (**2**): these systems can be obtained through a template process in which a metal center (e.g. $Co^{III}$) addresses the condensation of 11 fragments (three molecules of ethylenediamine, six molecules of formaldehyde, and two molecules of a triprotic acid, which act as capping units: ammonia for **1** and nitromethane for **2**). The sexidentate cage provides a pseudooctahedral coordinative environment, and it is so tightly bound to its guest that the metal can be extracted only under extremely drastic conditions (e.g. for cage **2**: (1) reduction of the very inert $Co^{III}$ ion to the labile oxidation state $Co^{II}$; (2) boiling in concentrated HBr or in aqueous NaCN).[4] This is the method by which to obtain the free ligand, which can incorporate further metal ions, giving complex species that are particularly sluggish with respect to demetalation.

The other important class of polyamine cages is that of the *bistrens*, in which two tripodal tetramine subunits of the *tren* type (tren: 2,2′,2″-triaminotriethylamine) are linked through their peripheral amine groups by three spacers R. The nature of R (an aliphatic chain, e.g. **3**, a xylyl group, e.g. **4**) determines the dimensions of the ellipsoidal cavity and controls the rigidity of the system. Bistren cages were first designed to host polyatomic anions, in particular those having a rodlike shape, e.g. $N_3^-$.[5] In order to provide electrostatic binding, some amine groups of the cage have to be protonated (typically the six secondary ones), and the selectivity of the receptor−substrate interactions depends on the matching of the length of the anion with that of the cavity (linear recognition).[6]

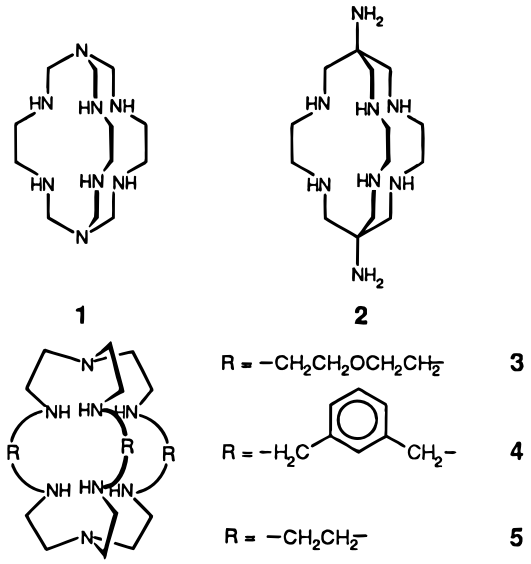


Bistren cages have also been designed to host pairs of transition metal ions, each metal (e.g. $Cu^{II}$) occupying a tetramine compartment. Given the stereochemical arrangement imposed by each tren subunit, a trigonal bipyramidal structure can be assumed, with one of the axial positions of the bipyramid exposed to the coordination of a further ligand. Thus, ambidentate polyatomic anions can bridge the two metal centers, giving rise to a stable adduct (a *cascade* complex).[7] It has been

⊗ Abstract published in *Advance ACS Abstracts*, February 1, 1997.

(1) (a) Università di Pescara. (b) Chimica Generale, Università di Pavia. (c) Centro Grandi Strumenti, Università di Pavia.
(2) Creaser, I. I.; Harrowfield, J. MacB.; Herlt, A. J.; Sargeson, A. M.; Springborg, J.; Geue, R. J.; Snow, M. R. *J. Am. Chem. Soc.* **1977**, *99*, 3181.
(3) Geue, R. J.; Hambley, T. W.; Harrowfield, J. MacB.; Sargeson, A. M.; Snow, M. R. *J. Am. Chem. Soc.* **1984**, *106*, 5478.
(4) Bottomley, G. A.; Clark, I. J.; Creaser, I. I.; Engelhardt, L. M.; Geue, R. J.; Hagen, K. S.; Harrowfield, J. M.; Lawrance, G. A.; Lay, P. A.; Sargeson, A. M.; See, A. J.; Skelton, B. W.; White, A. H.; Wilner, F. R. *Aust. J. Chem.* **1994**, *47*, 143.
(5) Dietrich, B.; Guilhem,J.; Lehn, J.-M.; Pascard, C.; Sonveaux, E. *Helv. Chim. Acta*, **1984**, *67*, 91.
(6) Lehn, J.-M. *Supramolecular Chemistry*; VCH: Weinheim, Germany, 1995; p 32.
(7) Motekaitis, R. J.; Rudolph, P. R.; Martell, A. E.; Clearfield, A. *Inorg. Chem.* **1989**, *28*, 112. Menif, R.; Reibenspies, J.; Martell, A. E. *Inorg. Chem.* **1991**, *30*, 3446.

S0020-1669(96)00933-0 CCC: $14.00 

recently shown that the dicopper(II) complex of the bistren cage bearing 1,3-xylyl spacers, **4**, displays a sharp selectivity pattern for the encapsulation of polyatomic anions, recognizing neither their shape nor their coordinating tendencies but simply their anion bite (i.e. the distance between two proximate donor atoms).[8]

In the smallest cage of the bistren family, **5**, the two tetramine compartments are linked through ethylene spacers. As an anion receptor, **5** possesses a spheroidal cavity and, in its six-protonated form, is the perfect host of the smallest spherical anion: fluoride.[9] Recently, inclusion of $F^-$ by **5** in aqueous solution has been investigated by potentiometry and NMR spectroscopy.[10] As far as metal inclusion is concerned, molecular models indicate that the bistren system **5** has too small a cavity to include a pair of metal ions, but **5** is able to incorporate two $Cu^{II}$ ions. However, the system is unstable, probably because there is no space for an anion to interface between the two metal centers, which spontaneously reduce to the +1.5 oxidation state (the solvent, water or methanol, acting as a reducing agent) and give rise to a novel type of metal−metal interaction.[11]

We were interested in verifying the coordinating tendencies of **5** as a mononucleating ligand. Structurally, **5** does not appear so different from sepulchrate **1**, both cages presenting a central tris(ethylenediamine) donor set, available for a coordination varying from octahedral to trigonal-prismatic. However, **5** exhibits different caps than sepulchrand. In particular, whereas the apical nitrogen atoms of **1** point their lone pairs outward, those of **5** point toward the cavity and are available for the coordination to the metal. The 1:1 complex of **5** with $Pb^{II}$ has been isolated and structurally characterized though X-ray diffraction studies.[12] The metal occupies the center of the cavity and seems to interact with all eight nitrogen atoms. A preliminary crystal structure of the $Co^{II}$ complex of the Schiff base precursor of **5** showed that the metal is coordinated by the six imine groups according to a distorted octahedral stereochemistry.[13]

We report here an investigation of the complexing tendencies of **5** toward the transition metal ions $Ni^{II}$ and $Cu^{II}$. We have found that metal inclusion into the cage in aqueous solution is a fast and reversible process and that several species of varying stoichiometry may coexist at equilibrium. Interestingly, in some metal complexes the cage has one or two amine groups protonated. In particular, a $Ni^{II}$ complex of the monoprotonated cage was obtained in a crystalline form, and its structure was determined through X-ray diffraction studies.

In contrast to what is observed with metal sepulchrates, the $Ni^{II}$ and $Cu^{II}$ complexes of **5** demetalate in acidic solution over the time scale of the stopped-flow experiment. The protonation of some uncoordinated nitrogen atoms of the cage appears to be the key step of the demetalation process.

## Experimental Section

Cage **5**, L, was prepared by the one-pot condensation of tren and glyoxal (2:3 ratio) in ethanol and subsequent reduction of the C=N bond by $NaBH_4$ in methanol.[14] Ligand **5** was recrystallized from water, satisfactorily analyzed, and used in equilibrium studies.

**$[Ni^{II}(LH)](ClO_4)_3$.** A 300 mg sample of L (**5**) was dissolved in a minimum amount of ethanol in an open beaker at room temperature and an equimolar amount of an aqueous solution of $Ni(ClO_4)_2$ was added under stirring. On addition of a saturated aqueous solution of $NaClO_4$ (~7 M) to the pale blue-violet solution, crystals of the $[Ni^{II}(LH)](ClO_4)_3$ complex salt separated as blue-violet plates. The product was filtered, washed twice with ethanol, and dried *in vacuo*. The complex salt was crystallized from ethanol/water saturated with $NaClO_4$. Anal. Calcd for $C_{18}H_{43}N_8Cl_3NiO_{12}$: C, 25.43; H, 4.98; N, 13.36. Found: C, 25.79; H, 5.55; N, 13.36. Crystals suitable for X-ray investigation were obtained by slow evaporation of an ethanolic solution in a beaker covered with filter paper.

**Equilibrium Studies.** Potentiometric titrations in both the absence and presence of metal ions ($Ni^{II}$, $Cu^{II}$, $Zn^{II}$) were carried out using an automatic system controlled by a personal computer and consisting of (i) a Radiometer PHM84 research pH-meter, equipped with a G202B Radiometer glass electrode, and an Ingold saturated sodium chloride calomel reference electrode; (ii) a Radiometer ABU80 Autoburette; (iii) a Metrohm thermostated cell; and (iv) an HETO thermostat. The temperature was kept to 25.00 ± 0.05 °C, and each titration was performed on a solution of 50 $cm^3$ made up to 0.1 M in $NaClO_4$. Typical concentrations of the ligand and the metal ion were $10^{-3}$ M. The electrode potential was calibrated by the method of Gran,[15] which gave also a $pK_W = 13.76$. The concentration of hydrogen ions was actually measured, thus pH should be rather considered as $-\log[H^+]$. Potentiometric titration curves (pH vs mL of titrant added, e.g. standard NaOH) were fitted by a least-squares nonlinear procedure, using the HYPERQUAD program.[16] For each investigated metal, a minimum of three titration experiments were carried out and each titration consisted of 50 to 100 points. Errors listed in Table 2 are those calculated by the HYPERQUAD program.

**Kinetic Studies.** The kinetic studies of the acid-catalyzed dissociation of $[M^{II}L]^{2+}$ (M= Cu and Ni) were performed using a high-speed diode array spectrophotometer coupled to a stopped-flow system. The spectrophotometer was a TIDAS (transputer integrated diode array system) apparatus, manufactered by J&M GmbH, Aalen, Germany. The 512-diode array can acquire a 512 point spectrum (range 200−620 nm) in a time as short as 1.3 ms, with a wavelength resolution of 0.8 nm. Up to 1000 spectra can be acquired and stored in the memory of the transputer board. The stopped-flow module associated to the spectrophotometer (SMF-3, Bio-Logic, Claix, France) consisted of a three-syringe system with two mixers. The three syringes are driven by independent stepping motors, operating at 6400 steps per motor turn. The observation chamber was a quartz cuvette with an optical path of 5 mm (SMF-3 TC-50/10). The movement of the syringes, the flow rate, and the flow stop, as well as fast spectral acquisition, were controlled by a 486/66 personal computer through dedicated software. The SMF-3 module was thermostated at 25.0 °C by circulating water. In a typical experiment, syringe 1 contained an $M^{II}L(ClO_4)_2$ solution prepared by mixing equimolar amounts of L and $M^{II}(ClO_4)_2$, and adjusted to pH = 10.5 with a standard solution of NaOH, and syringe 3 contained an $HClO_4$ solution, adjusted to a constant ionic strength with $NaClO_4$. The flow rate of each syringe was 4.00 mL $s^{-1}$, thus, the total flow rate after mixing was 8.00 mL $s^{-1}$. At this flow rate, the time the solution takes to travel from the mixer to the observation chamber (dead time) is about 3 ms.

**Crystal Data and Single-Crystal Structure Refinement.** Unit cell parameters and intensity data were obtained on Enraf-Nonius CAD-4 diffractometer. Calculations were performed with the MolEN program[17]


(8) Fabbrizzi, L.; Pallavicini, P.; Perotti, A.; Parodi, L.; Taglietti, A. *Inorg. Chim. Acta* **1995**, *238*, 5.
(9) Dietrich, B.; Lehn, J.-M.; Guilhem, J.; Pascard, C. *Tetrahedron Lett.* **1989**, *30*, 4125.
(10) Reilly, S. D.; Khalsa, G. R. K.; Ford, D. K.; Brainard, J. R.; Hay, B. P.; Smith, P. H. *Inorg. Chem.* **1995**, *34*, 569.
(11) (a) Barr, M. E.; Smith, P. H.; Antholine, W. E.; Spencer, B. *J. Chem. Soc., Chem. Commun.* **1993**, 1649. (b) Harding, C.; Nelson, J.; Symons, M. C. R.; Wyatt, J. *J. Chem. Soc., Chem. Commun.* **1994**, 3499−2500. (c) Farrar, J. A.; McKee, V.; Al-Obaidi, A. H. R.; McGarvey, J. J.; Nelson, J.; Thomson, A. J. *Inorg. Chem.* **1995**, *34*, 1302.
(12) Martin, N.; McKee, V.; Nelson, J. *Inorg. Chim. Acta* **1994**, *218*, 5.
(13) Hunter, J.; Nelson, J.; Harding, C.; McCann, M.; McKee, V. *J. Chem. Soc., Chem. Commun.* **1990**, 1148.
(14) Smith, P. H.; Barr, M. E.; Brainard, J. R.; Ford, D. K.; Freiser, H.; Muralidharan, S.; Reilly, S. D.; Ryan, R. R.; Silks, L. A., III; Yu, W. *J. Org. Chem.* **1993**, *58*, 7939.
(15) Gran, G. *Analyst* **1952**, *77*, 661.
(16) Sabatini, A.; Vacca, A.; Gans, P. *Coord. Chem. Rev.* 1992, **120**, 389.
(17) *MolEN, An Interactive Structure Solution Procedure*; Enraf-Nonius: Delft, The Netherlands, 1990.

**Table 1.** Crystal and Refinement Data for the Complex $[Ni^{II}(LH)](ClO_4)_3$ (L = **5**)

formula: $(C_{18}H_{42}N_8)Ni^{2+}\cdot 2ClO_4^-\cdot HClO_4\cdot H_2O$
$M_w = 746.30$
crystal color: violet
crystal dimenss: 0.33 × 0.32 × 0.22 mm
system: orthorhombic
space group: *Pbca*
$a = 14.173(2)$ Å
$b = 14.383(1)$ Å
$c = 30.622(3)$ Å
$\alpha, \beta, \gamma = 90°$
$V = 6242(1)$ Å$^3$
$Z = 8$
$D_{calc} = 1.589$ Mg m$^{-3}$
Radiation: Cu Kα ($\lambda = 1.541\,84$ Å) graphite monochromated
$\mu = 39.39$ cm$^{-1}$
T = 20(2) °C
$\theta$ range = 2−70°
scan type: $\omega-2\theta$
scan speed: 5.5 min$^{-1}$
scan width: (0.90+0.14 tan $\theta$)°
Reflcn measd: $0 < h < 17$; $-4 < k < 17$; $0 < l < 37$
transmn Coeff: $T_{min} = 0.785$; $T_{max} = 0.998$
max. decay: 16.9%
tot. no. of reflcns Measd: 7470
no. of unique reflcns: 5417
no. of $R_{int}$ 0.019
no. of obs. reflcns [$I > 3\sigma(I)$]: 4007
$R^a = 0.049$
GOF = 2.51
$R_w$ (w = $1/\sigma(Fo)^2$)$^b$ = 0.054
no. of refined params: 424
(shift/e.s.d.)$_{max}$: 0.3

$^a$ $R = \sum||F_o| - |F_c||/\sum|F_o|$. $^b$ $R_w = [\sum w(|F_o| - |F_c|)^2/\sum w(F_o)^2]^{1/2}$.

**Table 2.** Equilibrium Constants for Protonation and Complex Formation of the Octamine Cage **5** (L), in Aqueous 0.1 M $NaClO_4$, at 25 °C

| equilibrium | log $K$ |
|---|---|
| $L + H^+ = LH^+$ | 10.52 ± 0.01 |
| $LH^+ + H^+ = LH_2^{2+}$ | 9.56 ± 0.01 |
| $LH_2^{2+} + H^+ = LH_3^{3+}$ | 7.79 ± 0.02 |
| $LH_3^{3+} + H^+ = LH_4^{4+}$ | 5.63 ± 0.02 |
| $LH_4^{4+} + H^+ = LH_5^{5+}$ | 2.52 ± 0.04 |
| $LH_5^{5+} + H^+ = LH_6^{6+}$ | 1.72 ± 0.07 |
| $Ni^{2+} + LH^+ = [Ni(LH)]^{3+}$ | 7.03 ± 0.06 |
| $Ni^{2+} + L = [Ni(L)]^{2+}$ | 9.72 ± 0.02 |
| $Cu^{2+} + LH_2^{2+} = [Cu(LH_2)]^{4+}$ | 10.45 ± 0.05 |
| $Cu^{2+} + LH^+ = [Cu(LH)]^{3+}$ | 16.81 ± 0.02 |
| $Cu^{2+} + L = [Cu(L)]^{2+}$ | 18.07 ± 0.01 |
| $Zn^{2+} + LH_2^{2+} = [Zn(LH_2)]^{4+}$ | 7.59 ± 0.08 |
| $Zn^{2+} + LH^+ = [Zn(LH)]^{3+}$ | 11.07 ± 0.03 |
| $Zn^{2+} + L = [Zn(L)]^{2+}$ | 12.68 ± 0.02 |

on a MicroVax-3100 computer. The cell dimensions were determined by least-squares fitting of 25 centered reflections monitored in the range $35° < \theta < 40°$. Correction for *Lp*, intensity variation, and empirical absorption[17,18] were applied.

Pertinent experimental details are given in Table 1. The structure was solved by direct-methods (SIR88).[19] A table of the atomic coordinates is deposited in the Supporting Information. The non-hydrogen atoms were refined anisotropically by full-matrix least-square methods. Perchlorate oxygen atoms O7, O8, and O11 are disordered: alternative positions O7′, O8′, O11′ were observed, inserted in the model, and refined anisotropically; the relative occupancies are indicated in Table 2. All the hydrogen atoms were found in the difference Fourier map, inserted with an overall atomic displacement parameter equal to 4.0 Å$^2$, but not refined. Secondary extinctions[20] were applied. Atomic scattering factors were taken from the literature.[21] Diagrams of the molecular structure were performed by using the ORTEP program.[22]

## Results and Discussion

**1. Complex Formation in Aqueous Solution.** The coordinating tendencies of **5** toward metal ions was investigated by carrying out pH-metric titration experiments in aqueous 0.1 M $NaClO_4$, at 25 °C. In particular, pH vs *B*/*L* plot (*B* = equivalents of standard base added, e.g. NaOH, *L* = equivalents of **5**) were obtained for a solution containing: (a) **5** and excess acid; (b) **5**, 1 equiv of $Ni^{II}$, excess acid; (c) **5**, 1 equiv of $Cu^{II}$, excess acid; (d) **5**, 1 equiv of $Zn^{II}$, excess acid. *B*/*L* = 0 corresponds to the situation in which all the ammonium groups of the cage have been titrated. The corresponding titration profiles are deposited in the Supporting Information.

The octamine cage **5** takes up as many as six protons in the investigated pH range (2-12). The log $K_i$ values compare fairly well with those previously reported.[10] A serious discrepancy refers to log $K_1$ (present work, 0.1 M $NaClO_4$, 10.52; literature, 0.1 M $NaNO_3$, 11.18). Difference can be only in part ascribed to the variation of ionic background. In any case, both in $NaClO_4$ and $KNO_3$ media, the highest protonated form was $LH_6^{6+}$, at pH = 2. It should be noted that the reference tripodal tetramine *tren* takes up three protons. It is suggested that the triprotonated species $trenH_3^{3+}$ has the three peripheral nitrogen atoms protonated: the protonation of the central tertiary amine group is prevented by strong electrostatic repulsions exerted by the peripheral ammonium groups. Such repulsive effects are much stronger in the constrained bistren system **5**. In fact, only log $K_1$ and log $K_2$, which should refer to the protonation of nitrogen atoms of the two subunits, show comparable values to those of tren (tren: log $K_1$ = 10.42, log $K_2$ = 9.88, log $K_3$ = 8.91).[23] From the third step onwards, the proton affinity of **5** decreases substantially. In particular, the fifth and sixth protons are taken up at pH ≅ 2. It is probable that in the aqueous $LH_6^{6+}$ species, the protons are bound to the six secondary nitrogen atoms. This situation has been observed in the crystalline $\{LH_6^{6+}, F^-\}$ inclusion complex[9] and has been also suggested on the basis of NMR titration experiments.[10]

Least-squares fitting of the titration curve in presence of 1 equiv of $Ni^{II}$ indicated the formation of two major species: $[Ni^{II}(LH^+)]^{3+}$ and $[Ni^{II}(L)]^{2+}$. The $[Ni^{II}(LH^+)]^{3+}$ complex begins to form at pH = 5.5 and reaches the respectable concentration of 70% at pH = 7. Then the $[Ni^{II}(L)]^{2+}$ species forms and is present at 100% from pH = 9. The corresponding distribution curve (% abundance vs pH) is deposited in the Supporting Information. The predominance of the $[Ni^{II}(LH^+)]^{3+}$ complex in the neutral solution has to be associated with the relatively poor stability of the $[Ni^{II}(L)]^{2+}$ species. In particular, it should be noted that the log $K_{ML}$ value (which refers to the equilibrium $Ni^{2+} + L = [Ni^{II}(L)]^{2+}$) is 5 log units lower than that for the $[Ni^{II}(tren)]^{2+}$ complex (log $K$ = 14.95).[23] This situation appears surprising, if one considers that **5** offers eight donor atoms for coordination and that the preferred coordination number of $Ni^{II}$ is six. Notice that such a number can be achieved in the tren complex through the coordination of two solvent molecules: $[Ni^{II}(tren)(H_2O)_2]^{2+}$.[24] The poor stability

(18) North, A. C. T.; Phillips, D. C.; Mathews, F. S. *Acta Crystallogr.* **1968**, *A24*, 351.
(19) Burla, M. C.; Camalli, M.; Cascarano, G.; Giacovazzo, G.; Polidori, G.; Spagna, R.; Viterbo, D. *J. Appl. Crystallogr.* **1989**, *22*, 389.
(20) Zachariasen, W. H. *Acta Crystallogr.* **1963**, *A16*, 1139.
(21) *International Tables for X-ray Crystallography*; Kynoch Press: Birmingham, England, 1974, Vol. 4, pp 99−101 and 149−150.
(22) Johnson, C. K. *ORTEP*; Report ORNL-3794; Oak Ridge National Laboratory, Oak Ridge, USA, 1976.
(23) Anderegg, G.; Gramlich, V. *Helv. Chim. Acta* **1994**, *77*, 685. Protonation constants of *tren* have been recently reported also by: Canary, J. W., Xu, J.; Castagnetto, J. M.; Rentzeperis, D.; Marky, L. A. *J. Am. Chem. Soc.* **1995**, *117*, 11545.

of the $[Ni^{II}(\mathbf{5})]^{2+}$ complex is probably connected to the polycyclic nature of the ligand framework, which does not allow the donor atoms to establish strong interactions with the metal center for an octahedral coordination arrangement.

In the case of copper, the complex with the diprotonated ligand, $[Cu^{II}(LH_2^{2+})]^{4+}$, forms at a little below pH 3, reaching its maximum concentration at pH = 3.5. Then, the major species $[Cu^{II}(LH^{+})]^{3+}$ forms and is present at 100% in the 4-8 pH range. The complex of the neutral ligand $[Cu^{II}(L)]^{2+}$ predominates only in a rather alkaline solution (pH > 10). The corresponding distribution curve (% abundance vs pH) is deposited in the Supporting Information. The greater importance of complexes involving protonated forms of the cage observed for copper can be ascribed to the preference of this metal center for coordination numbers lower than 6. The versatile coordinating tendencies of $Cu^{II}$ may also explain the fact that log $K_{ML}$ has a value comparable to that observed for the formation of $[Cu^{II}(tren)]^{2+}$ (log $K$=19.58).[23] In particular, it seems that the stereochemically versatile $Cu^{II}$ ion adjusts well to the coordinative framework of **5**. The formation of the $Cu^{1.5+}-Cu^{1.5+}$ species under the present conditions (1:1 cage to metal ratio, pH around 10, 25 °C) can be excluded in view of the absence of any intense absorption band in the 600−750 nm interval.[11a]

It should also be noted that the less stereochemically demanding $Zn^{II}$ ion displays a behavior quite similar to that of the genuine transition metals $Ni^{II}$ and $Cu^{II}$. In fact, the complex of the diprotonated cage $[Zn^{II}(LH_2^{2+})]^{4+}$ forms at pH = 5 and reaches a concentration of 50% around pH = 6; then, the monoprotonated complex $[Zn^{II}(LH^{+})]^{3+}$ is present as the major species over a substantial pH range (7−9). The neutral ligand complex $[Zn^{II}(L)]^{2+}$, which is the dominating species at pH ≥ 9, shows a lower solution stability than the $[Zn^{II}(tren)]^{2+}$ system (log $K$ = 15.00),[23] and this can again be ascribed to the constrained nature of the octamine ligand framework. The corresponding distribution curve (% abundance vs pH) is deposited in the Supporting Information.

The existence in solution of stable $[M^{II}(LH^{+})]^{3+}$ complexes for all the investigated metals is puzzling and contrasts with the hypothesis that cage **5** adopts a coordination mode similar to that of the classical sepulchrand **1**, i.e. involving the six secondary nitrogen atoms of the "tris(ethylenediamine)" core. A more direct insight into the coordinating tendencies of the cage and the nature of the monoprotonated species comes from the crystal and molecular structure of the $[Ni^{II}(LH^{+})]^{3+}$ complex.

**2. Molecular Structure of the $[Ni^{II}(LH^{+})]^{3+}$ Complex.** Crystals of the $[Ni^{II}(LH^{+})](ClO_4)_3$ salt were obtained through crystallization of a solution of the complex at pH = 7. The asymmetric unit contains three perchlorate ions and one cationic complex in which the one noncoordinated amine is protonated and hydrogen-bonded to a water molecule. A perspective view of the tripositive cationic complex is shown in Figure 1.

Selected bond lengths and selected bond angles and are given respectively in Tables 3 and 4. A table containing selected torsion angles and a table containing hydrogen-bonding interactions are deposited in the Supporting Information.

Of the eight potential donor atoms, one tertiary (N1), and five secondary amine groups (N2, N3, N5, N6, and N7) are coordinated to $Ni^{II}$, whereas the tertiary nitrogen atom, N4, and the secondary one, N8, are far away from the metal center (at distances of 3.522(3) and 5.074(3) Å, respectively). Of the two noncoordinated nitrogen atoms, N4 and N8, it is the latter that is protonated, as indicated by the following evidence: (i) the N8 atom is the farthest from the cation; (ii) two maxima interpretable as two hydrogen atoms were found in the difference Fourier map nearby the N8 atom, in positions compatible with strong hydrogen bonding interactions, and these interactions involve the water oxygen atom Ow and the perchlorate oxygen atom O6 as acceptors; (iii) the position of the N4 nitrogen atom allows one to exclude the possibility of any hydrogen-bonding interaction, and in any case no significative electronic density was observed in the vicinity of this atom.

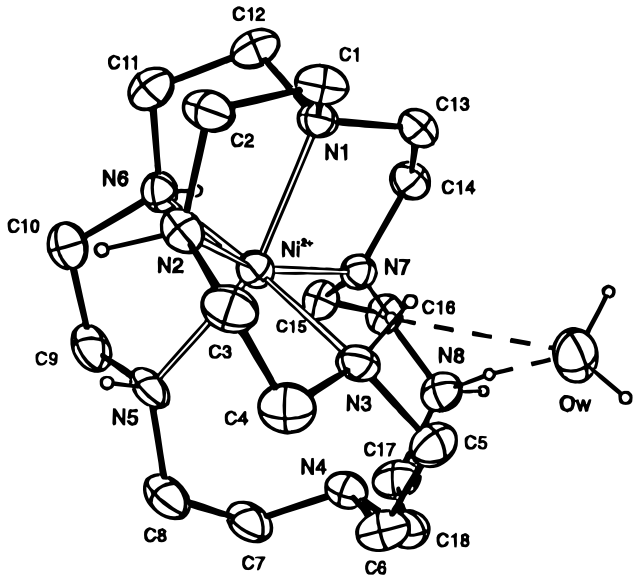


**Figure 1.** ORTEP view of the tripositive complex $[Ni^{II}(LH^{+})]^{3+}$ (L = **5**); 30% probability ellipsoids are shown.

The $Ni^{II}$ ion is coordinated in a very distorted octahedral arrangement, with the N−Ni−N angles varying in the ranges 78.2(1)−100.4(1) and 158.2(2)−176.6(1)°. All the Ni−N bond distances are not too much larger than those expected for a hexamine $Ni^{II}$ complex, with the exception of the especially large Ni−N2 distance (2.239(4) Å). Both the distorted octahedral geometry and the electrostatic repulsion between the metal center and the ammonium group are expected to induce a conformational and geometrical strain in the cage framework. Indeed, the complex appears seriously strained, as shown by the following structural features: (i) the significant deviation of some torsion angle values from those expected for an *anti* (180°) or a *gauche* (60°) conformation; (ii) the unusually large value of some N−C−C bond angles (N3−C5−C6, 114.9(4)°; N4−C7−C8, 116.3(4)°; N5−C8−C7, 117.1(4)°; N7−C15−C16, 116.5(4)°). On the other hand, the C−N−C angles for both coordinated and noncoordinated nitrogen atoms exhibit values in agreement with $sp^3$ hybridization, with three exceptions: C10−N6−C11, 116.6(3)°; C14−N7−C15, 113.4(3)°; C16−N8−C17, 116.6(4)°.

A figure showing the hydrogen-bonding network is deposited in the Supporting Information. The strongest interactions are (i) those involving the H-atoms on the protonated amine group N8, which are directed toward the water oxygen atom Ow and the perchlorate oxygen atom O6, and (ii) those involving the water molecule as a donor toward the perchlorate oxygen atoms O9 and $O8^{ii}$ (see Table 2 for complete H-bond description and symmetry codes). The molecular folding of the cage ligand does not permit the formation of intramolecular hydrogen bonds between the amine groups and the oxygen atoms of the perchlorate ion and water. On the other hand, perchlorate ions play an essential role in the crystal packing, by connecting neighboring metal complexes in the cell.

(24) Barbucci, R.; Paoletti, P.; Fabbrizzi, L. *Inorg. Chim. Acta Rev.* **1973**, *7*, 43.

**Table 3.** Selected Bond Lengths (Å) for the Complex $[Ni^{II}(LH)](ClO_4)_3$ (L = **5**)

| | | | | | | | |
|---|---|---|---|---|---|---|---|
| Ni−N1 | 2.127(4) | Ni−N2 | 2.239(4) | N5−C9 | 1.488(6) | N6−C10 | 1.483(6) |
| Ni−N3 | 2.183(3) | Ni−N5 | 2.185(4) | N6−C11 | 1.467(6) | N7−C14 | 1.491(6) |
| Ni−N7 | 2.171(3) | Ni−N6 | 2.099(3) | N7−C15 | 1.486(5) | N8−C16 | 1.501(6) |
| N1−N4 | 3.522(3) | Ni−N8 | 5.074(3) | C1−C2 | 1.517(6) | C3−C4 | 1.488(6) |
| N2−C3 | 1.498(6) | N2−C2 | 1.480(6) | C5−C6 | 1.517(7) | C7−C8 | 1.527(7) |
| N3−C4 | 1.502(5) | N3−C5 | 1.486(5) | C9−C10 | 1.491(7) | C11−C12 | 1.523(7) |
| N4−C6 | 1.485(5) | N4−C7 | 1.472(6) | C13−C14 | 1.515(6) | C17−C18 | 1.523(6) |
| N4−C18 | 1.491(6) | N5−C8 | 1.490(6) | | | | |

**Table 4.** Selected Bond Angles (deg) for the Complex $[Ni^{II}(LH)](ClO_4)_3$ (L = **5**)

| | | | | | | | |
|---|---|---|---|---|---|---|---|
| N1−Ni−N2 | 80.5(1) | N1−Ni−N3 | 100.4(1) | Ni−N1−C1 | 108.4(3) | N3−C4−C3 | 109.3(4) |
| N1−Ni−N5 | 161.1(1) | N1−Ni−N6 | 81.6(1) | Ni−N1−C12 | 110.1(3) | N3−C5−C6 | 114.9(4) |
| N1−Ni−N7 | 82.0(1) | N3−Ni−N5 | 96.4(1) | Ni−N1−C13 | 105.5(2) | N4−C6−C5 | 112.4(4) |
| N2−Ni−N3 | 78.2(1) | N3−Ni−N6 | 176.6(1) | C1−N1−C12 | 110.0(3) | N4−C7−C8 | 116.3(4) |
| N2−Ni−N5 | 94.6(1) | N3−Ni−N7 | 92.3(1) | C1−N1−C13 | 111.7(3) | N5−C8−C7 | 117.1(4) |
| N2−Ni−N6 | 99.5(1) | N5−Ni−N6 | 81.2(1) | C12−N1−C13 | 111.0(3) | N5−C9−C10 | 109.6(4) |
| N2−Ni−N7 | 158.2(1) | N6−Ni−N7 | 90.7(1) | Ni−N2−C2 | 108.1(2) | N6−C10−C9 | 108.9(4) |
| N5−Ni−N7 | 106.1(1) | Ni−N5−C8 | 129.6(3) | Ni−N2−C3 | 110.0(2) | N6−C11−C12 | 108.8(4) |
| C6−N4−C18 | 108.0(3) | Ni−N5−C9 | 107.2(3) | C2−N2−C3 | 109.8(3) | N1−C12−C11 | 111.4(4) |
| C7−N4−C18 | 107.8(3) | C8−N5−C9 | 111.7(3) | Ni−N3−C4 | 104.5(3) | N1−C13−C14 | 111.2(3) |
| Ni−N6−C10 | 109.3(3) | C10−N6−C11 | 116.6(3) | Ni−N3−C5 | 127.9(2) | N7−C14−C13 | 109.8(3) |
| Ni−N6−C11 | 108.8(2) | C14−N7−C15 | 113.5(3) | C4−N3−C5 | 111.9(3) | N7−C15−C16 | 116.5(4) |
| Ni−N7−C14 | 109.4(2) | C16−N8−C17 | 116.6(4) | C6−N4−C7 | 111.6(3) | N8−C17−C18 | 113.6(4) |
| Ni−N7−C15 | 116.4(3) | N2−C2−C1 | 110.0(3) | N4−C18−C17 | 115.0(4) | N8−C16−C15 | 112.9(3) |
| N1−C1−C2 | 109.5(3) | N2−C3−C4 | 111.6(3) | | | | |

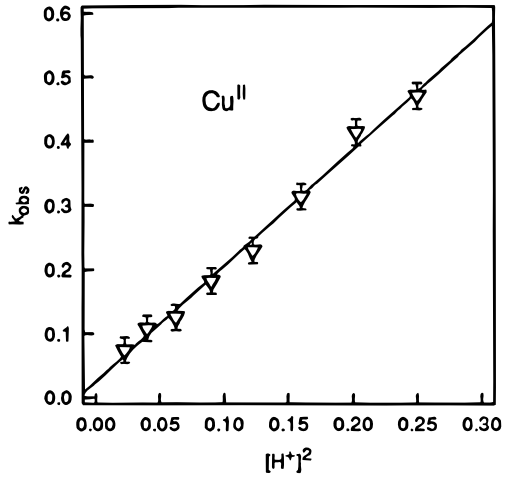


**Figure 2.** Demetalation of $[Cu^{II}L]^{2+}$ in aqueous $HClO_4$, at 25 °C with the dependence of the rate constants on the hydrogen ion concentration shown.

**3. Kinetic Investigation of the Demetalation Process in Acidic Solution.** Both $[Ni^{II}(L)]^{2+}$ and $[Cu^{II}(L)]^{2+}$ complexes are labile with respect to demetalation in acidic solution, as demonstrated by the instantaneous decoloration of the violet and blue solution, respectively, on addition of strong acid. Thus, acid dissociation of the complexes had to be followed by stopped-flow spectrophotometry using a diode array apparatus. In the case of the $Cu^{II}$ complex, one of the syringes contained an $HClO_4$ solution of between 0.15−0.5 M, adjusted to $I = 0.5$ M with $NaClO_4$ and the other syringe a $1.5 \times 10^{-3}$ M solution of the metal complex. The demetalation process was followed through the decrease of the absorption band centered at 300 nm. First-order dependence on the metal complex was observed. The $k_{obs}$ vs $[H^+]$ plot is not linear, but a good fit may be obtained by plotting $k_{obs}$ vs $[H^+]^2$ (see Figure 2), the slope of the plot $k_H$ ($=k_{obs}[H^+]^{-2}$) having a value of $1.81 \pm 0.06$ $M^{-2}$ $s^{-1}$.

The second-order dependence on $[H^+]$ indicates that two protons participate in the transition state of the reaction. Thus, the kinetic behavior of $[CuL]^{2+}$ in acidic solution can be described in terms of eqs 1-5. The first two steps involve the protonation of uncoordinated nitrogen atoms of the cage,

$$[CuL]^{2+} + H^+ \overset{K_1}{\longleftrightarrow} [Cu(LH^+)]^{3+} \quad (1)$$

$$[Cu(LH^+)]^{3+} + H^+ \overset{K_2}{\longleftrightarrow} [Cu(LH_2{}^{2+})]^{4+} \quad (2)$$

$$[Cu(LH_2{}^{2+})]^{4+} + H^+ \overset{K_3}{\longleftrightarrow} [Cu(LH_3{}^{3+})]^{5+} \quad (3)$$

$$[Cu(LH_3{}^{3+})]^{5+} + H^+ \overset{K_4}{\longleftrightarrow} [Cu(LH_4{}^{4+})]^{6+} \quad (4)$$

$$[Cu(LH_4{}^{4+})]^{6+} \overset{k}{\rightarrow} Cu^{2+}(aq) + LH_4{}^{4+} \quad (5)$$

forming the stable species identified in the equilibrium studies: $[Cu(LH^+)]^{3+}$ and $[Cu(LH_2{}^{2+})]^{4+}$: it can be assumed that these stable species do not have significant dissociation rates and that protonation steps 1 and 2 are not directly involved in the dissociation kinetics. The third protonation step is expected to remove one of the coordinated amine group from the metal center, giving rise to the five-coordinate complex $[Cu(LH_3{}^{3+})]^{5+}$. Finally, on uptake of a further proton, the highly positively charged species $[Cu(LH_4{}^{4+})]^{6+}$ forms and undergoes decomposition, according to step 5.

The rate equation, (6), can be thus derived from eqs 3 to 5.

$$\text{rate} = \frac{kK_3K_4[CuLH_2{}^{4+}][H^+]^2}{1 + K_3[H^+] + K_3K_4[H^+]^2} \quad (6)$$

In this connection, it should be noted that $K_1$ and $K_2$ values can be obtained by the appropriate combination of the constants of the complex formation equilibria of Table 3 (they are $10^{9.26}$ and $10^{3.16}$, respectively). Then, we can reasonably assume that $K_3$ (and thus $K_4$), associated with the protonation of an amine group within a concave system that bears 4 (or 5) positive charges and also contains the $Cu^{2+}$ ion, will be much lower than $K_2$ and, in particular, $\ll 1$.

Then, we can assume that, under the conditions of the experiment, the term $K_3[H^+] + K_3K_4[H^+]^2$ is $\ll 1$. Then, if we put $k_H = kK_3K_4$, we obtain the reduced rate law:

$$\text{rate} = k_H[CuLH_2{}^{4+}][H^+]^2 \quad (7)$$

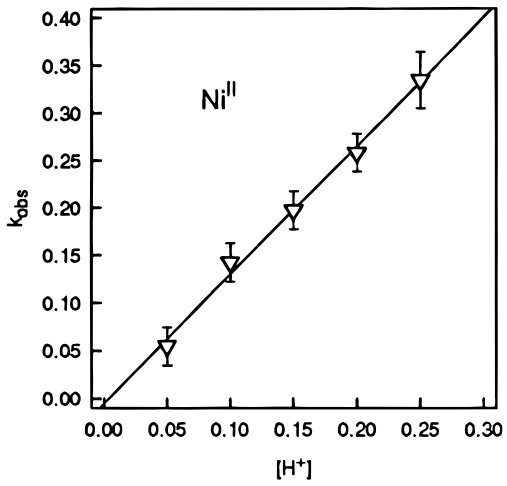


**Figure 3.** Demetalation of $[Ni^{II}L]^{2+}$ in aqueous $HClO_4$, at 25 °C, with the dependence of the rate constants on the hydrogen ion concentration shown.

Finally, if we assume that $[CuL^{2+}]_{tot} = [CuLH_2^{4+}]$, eq 7 fits well the $k_{obs}$ vs $[H^+]^2$ plot of Figure 2.

Dissociation of the $Ni^{II}$ complex was investigated under similar conditions, using $HClO_4$ solutions in the range 0.05−0.25 M, adjusted to $I = 0.25$ M with $NaClO_4$. Here too, we found a first-order dependence on the metal complex concentration, but $k_{obs}$ was found to increase linearly with $[H^+]$, giving a value of $k_H = k_{obs}[H^+]^{-1} = 1.35 \pm 0.05\ M^{-1}\ s^{-1}$ (see plot in Figure 3).

A similar kinetic treatment can be applied to the $Ni^{II}$ complex. The linear dependence of $k_{obs}$ upon $[H^+]$ would suggest that demetalation takes place following the protonation to the $[Ni^{II}(LH_3^{3+})]^{5+}$ complex, i.e. one step earlier than for the $Cu^{II}$ analogue.

$$[Ni^{II}(LH_3^{3+})]^{5+} \xrightarrow{k} Ni^{2+}(aq) + LH_3^{3+} \qquad (8)$$

On this assumption, the rate law should be reduced to:

$$\text{rate} = \frac{kK_3[NiLH_2^{4+}][H^+]}{1 + K_3[H^+]} \qquad (9)$$

Then, assuming that $K_3 \ll 1$, and putting $k_H = kK_3$, we obtain the reduced form of the rate law

$$\text{rate} = k_H[NiLH_2^{4+}][H^+] \qquad (10)$$

which fully accounts for the linear dependence of $k_{obs}$ upon $[H^+]$. Thus, for the $Ni^{II}$ cage complex, the protonation of only one of the coordinated amine groups is sufficient to promote the destruction of the complex. This may be due to the lower intrinsic stability of $Ni^{II}$ polyamine complexes than those of $Cu^{II}$ and to their lack of predisposition toward five-coordination.

## Conclusions

Octamines **1** and **5** have a similar shape—which accounts for the term *cage* being used for them—and differ in the number of methylene groups (one and two, respectively) linking the apical tertiary nitrogen atoms to the secondary nitrogen atoms of the ethylenediamine fragments. Moreover, it should be pointed out that the apical nitrogen atoms of **1** have an aminal nature, whereas those of **5** are amine groups. As a consequence, cages **1** and **5** display a strikingly different behavior with respect to the incorporated metal ions. For the smaller cage **1**, the metal is a prisoner which can be released only under forcing conditions; for the larger cage **5**, the metal is a welcome guest, free to come and go according to the pH of the solution. **5** offers a larger cavity than **1**, and the $N(CH_2CH_2-)_3$ caps of **5** ensure a relatively greater flexibility than the $N(CH_2-)_3$ cap of **1**. Whereas cavity size and flexibility can play an important role, we believe that the strikingly different behavior of the metal complexes of cages **1** and **5** has to be ascribed to the different nature of the apical nitrogen atoms in each. In cage **1**, the apical nitrogen atoms point their lone pairs away from the cavity and cannot be involved in the metal coordination; in **5**, the lone pairs point inward and can bind the metal. The latter possibility has been demonstrated by the crystal and molecular structure of the $[Ni(LH^+)]^{3+}$ complex, in which the metal center is displaced toward one end of the cavity and is bound to the apical tertiary nitrogen atom. We are not in the position to say whether on deprotonation of the $[Ni(LH^+)]^{3+}$ complex the metal ion remains coordinated to the same donor atoms or moves toward the center in order to profit from coordination by the tris(ethylenediamine) core. The two coordination topologies should not differ too much in energy and should not be separated by a large kinetic barrier: thus, the metal ion is expected to move easily within the cage cavity. Most importantly, in the $[M^{II}(\mathbf{5})]^{2+}$ complex, the two uncoordinated amine lone pairs encourage the ingress of protons into the cavity. Thus, following protonation, the electrostatic repulsions exerted by ammonium groups within the cavity further destabilize and deform the coordinative arrangement, promoting metal extrusion. Therefore, the lability of $[M^{II}(\mathbf{5})]^{2+}$ complexes toward demetalation in the presence of acid seems connected to the availability of basic sites within the cavity, a possibility precluded by the lack of similar sites in the corresponding complexes of **1** and **2**.

In conclusion, in contrast to the cages **1** and **2**, which offer space exclusively for the metal, **5** is an open enclosure which also offers room to some other small and invading visitors, protons, which in turn actively cooperate to dislodge the first guest, the metal ion.

**Acknowledgment.** This work has been supported by CNR (Progetto Strategico "Tecnologie Chimiche Innovative") and by the European Union, within the HCM program (Network Contract No. ERBCHRXCT940492).

**Supporting Information Available:** Tables of crystallographic parameters (atomic coordinates, anisotropic thermal parameters, bond lengths, bond angles, least squares planes, torsion angles, selected hydrogen bonding interactions), an ORTEP view of the crystal packing, a figure reporting a view of the hydrogen-bonding interactions, a figure containing the titration curves (pH vs B/L) of cage **5** in the absence and in the presence of $Ni^{II}$, $Cu^{II}$, and $Zn^{II}$ (1:1 metal to ligand ratio), and figures containing the distribution diagrams (% abundance vs pH) for the systems $Ni^{II}$/**5**, $Cu^{II}$/**5**, and $Zn^{II}$/**5** (19 pages). Ordering information is given on any current masthead page.

IC960933P